Alternating Current Conductivity and Spectroscopic Studies on Sol−Gel Derived, Trivalent Ion Containing Silicate−Tetra(ethylene glycol)-Based Composites

Sagar Mitra and S. Sampath*

Department of Inorganic and Physical Chemistry, Indian Institute of Science, Bangalore, India

Received July 30, 2004; Revised Manuscript Received October 26, 2004

ABSTRACT: Sol−gel derived, composite solid ionic conductors containing the triflate salt of europium-(III) in silicate−tetraethylene glycol matrices have been prepared. The ionic interactions in the matrix are followed using vibrational spectroscopy. The quantitative estimations of various species such as free ions, ion pairs, and aggregates in the organically modified electrolyte (ormolytes) suggest that the free ion concentration is considerably high. This is in contrast to the formation of large fractions of ion pair expected for high-valent cations with triflate. The ionic conductivity is found reach values of 10^{-3} S/cm at 80 °C. The temperature dependence of ionic conductivity is observed to follow pure Arrhenius-type behavior. The high-frequency ac impedance behavior of the ormolyte has been explained on the basis of the universal power law equation related to the "jump relaxation model" framework. The conductivity relaxation time, τ_{peak}, has been evaluated from the complex resistivity relaxation spectra. It is suggested that anion conduction predominates over cations at low temperatures while the trend is toward cation conduction at high temperatures.

I. Introduction

Polymer-based solid electrolytes comprising of an inorganic salt solubilized in a polymeric matrix have attracted wide interest due to their potential applications in solid-state rechargeable batteries, fuel cells, sensors, electrochromic display devices, and supercapacitors.[1,2] These electrolytes offer several advantages such as high ionic conductivity ($\sigma \approx 10^{-3}$ S cm^{-1}), lightweight, flexibility, amenability of thin-film formation, and wide electrochemical potential voltage window.[1] Most of the literature reports concern electrolytes containing either monovalent (mostly lithium salts) or divalent cations (Mg^{2+}, Zn^{2+}, etc.).[3−6] The trivalent cation-based solid electrolytes have not received considerable attention since they are relatively poor migrant species.[7−13] The high cationic charge leads to significant interactions with anionic species in the matrix, leading to charged and neutral pairs that reduce the ionic conductivity.[7−11] This is observed with even large anions such as triflates.[7,8] The studies related to the trivalent triflate-based polymer electrolytes also explore the possibility of developing materials in which luminescent behavior of the trivalent cation is exploited.[7−11] Lanthanide containing glassy oxide-based electrolytes have been developed as potential candidates for optoelectronics and solid-state laser materials.[10,11]

As for the polymeric host, ethylene oxide-based polymers have been very extensively studied for incorporating ionic salts to prepare solid electrolytes.[1] The mechanical stability of the polymeric and gel-based electrolytes are generally found to be poor. It is desirable to have solid electrolytes consisting of a relatively a rigid matrix along with a plasticizer for flexibility. The solid electrolytes should also exhibit good thermal and mechanical stability. There have been several attempts to improve the properties of solid electrolytes.[1] Addition of fine particles such as silica and alumina to a polymer host is one of the methods proposed and has resulted in limited success.[14−17] Sol−gel processing of materials has led to the flexibility of finely mixing organic moieties with inorganic matrices resulting in composites.[18] This will be similar to having inorganic fillers in an organic host. Several studies report good ionic conductivity for sol−gel-based solid electrolytes. Ravine and co-workers have reported ionic conductivities of the order of $\sigma \approx 7 \times 10^{-5}$ for sol−gel derived silicates containing lithium salts at ambient temperature.[18]

The third aspect of a polymer electrolyte is the ion transport property and the ionic interactions in the matrix. This has been extensively probed in poly-(ethylene oxide) (PEO)-based polymer matrices using a variety of vibrational spectroscopic and impedance techniques.[7,8,19−22] The investigations reveal that the conductivity mechanism involves two processes: one is an ion hop from one equivalent site to another, and the other is related to the polymer segmental motion that also assists ionic movement. It has been reported that in the high-frequency region there is a decrease in conductivity with a decrease in frequency and is attributed to the dielectric relaxation (dipolar relaxation) of the polymer backbone. In the low-frequency region, the conductivity is found to be independent of the frequency and is attributed to the dc conductivity resulting from the ion motion in the polymer matrix.[19,20] Recently, Di Noto[21,22] has extended the impedance measurements to the poly(ethylene glycol)-based systems [(PEG-400)−$(LiCl)_x$ and PEG400−$(MgCl_2)_x$] and correlated the ionic conductivity events with microscopic events in polymer matrix like polymer relaxation (segmental motion), relaxation of coordination sites, etc.

The present interest in solid electrolytes is toward the use of organic−inorganic composite matrices to solubilize trivalent cation containing salts. Earlier spectroscopic investigations involving trivalent cation containing solid electrolytes reveal the absence of free ions, and consequently ion pair has been observed as a major component, even at low salt concentrations in

* Corresponding author. E-mail: sampath@ipc.iisc.ernet.in.

10.1021/ma0484328 CCC: $30.25
Published on Web 12/07/2004

PEO-based electrolytes.[7,8] One of the main reasons ascribed to this observation is that the polymer is not able to solvate the trivalent cations, and as a result the species are present as ion pairs in the matrix. Hence, it is necessary to search for matrices that can give rise to solvated free ions as a major component and consequently exhibit high ionic conductivity. The sol−gel derived organically modified silicates containing ionic salts (ormolytes) may give rise to a different behavior based on the properties of organic−inorganic interfaces. The nature of charge carriers and the relative number of charge carriers that determine the total conductivity of the solid electrolyte may vary as well. In the present studies, the use of sol−gel derived silicates modified with poly(ethylene glycol) is explored as a matrix for europium triflate-based solid electrolyte. Ethylene glycol is expected to improve the dissociation and solvate the cations (ϵ of ethylene glycol is 10), and consequently high ionic conductivity may be observed. Triflate salts have been used to augment the dissociation based on the large size of the anion. We have used extensive vibrational spectroscopy to understand the dissociation and consequent ionic interactions in the matrix. Impedance spectroscopy in a wide frequency range is used to understand the behavior of the dielectric properties and the conductivity mechanism associated with the electrolyte.

II. Experimental Section

Materials. Tetraethoxysilane (TEOS), tetra(ethylene glycol) [$(PEG)_4$], europium trifluoromethanesulfonate [europium triflate, $Eu(CF_3SO_3)_3$], and potassium bromide (KBr) were the products of Aldrich. Double-distilled water was used in all the preparations.

Synthesis. The preparation of the solid electrolyte was based on a reported procedure to synthesize silicate network containing ethylene oxide functionalities.[23] Briefly, the preparation involved the addition of TEOS (4.9 mL) to $(PEG)_4$ (3.85 mL) and water (0.8 mL) with vigorous stirring. The mixture was heated to 60 °C and kept for 5 min. A calculated amount of europium salt [1.33 g for 0.72 M with respect to PEG] was then added and dissolved in the mixture. One drop of concentrated HCl was subsequently added to the turbid solution to catalyze the hydrolysis of the silane, and the mixture was vigorously stirred. After 10−15 min, the hydrolysis was completed and a single-phase solution was obtained. The mixture was then cast on a polypropylene Petri dish and kept in a vacuum oven at a temperature of 40 °C for 1−3 months depending upon the composition and the gelation time. Final curing of the cast and dried samples was carried out by slowly heating the samples from 60 to 90 °C over a period of 3 days and then kept at 60 °C for 2 days. The amounts given above correspond to $[1]_4[8]$ composition where the molar composition of {[PEG]/[TEOS]} = 1 and {[TEOS]/[salt]} = 8. The organically modified electrolytes (ormolytes) are denoted by the nomenclature $[X]_n[Y]$, where $[X]$ represents the molar ratio of [PEG]/[TEOS], n is chain length of the poly(ethylene glycol) unit (here $n = 4$), and $[Y]$ is the molar ratio of $[TEOS]/[M^{n+}]$. The samples were found to be transparent and mechanically stable, crack-free monoliths. Two different series of samples were prepared, and in each of these series only one of the parameters was varied (X or Y) while the other remained constant. The compositions prepared in the present studies are shown in Table 1. In this range, all the monoliths are thermally and mechanically stable. Beyond these limits, the monoliths are mechanically unstable, and phase separation is also observed in a few cases.

Experimental Techniques. FT-Raman spectra were recorded using a Bruker RFS-100/S FT-Raman spectrometer. The laser power used was 200 mW with a radiation spot of 0.1 mm diameter. An Nd:YAG laser with a source wavelength of 1.064 μm was used. The scattered light was collected at an angle of 180° to the incident light. Each spectrum was averaged over 500 scans, and the resolution was 2 cm^{-1}. A liquid nitrogen cooled germanium detector was used. All the solid electrolyte samples were finely ground to powder and then mounted on the stainless steel sample holder.

Table 1. Ormolyte Compositions Prepared in the Present Study[a]

composition	composition	salt
$[1]_4[100]$	$[1.5]_4[30]$	
$[1]_4[50]$	$[1.5]_4[20]$	
$[1]_4[30]$	$[1.5]_4[15]$	$Eu(CF_3SO_3)_3$
$[1]_4[20]$	$[1.5]_4[10]$	
$[1]_4[10]$	$[1.5]_4[8]$	
$[1]_4[8]$		

[a] The nomenclature is $[X]_4[Y]$, where X and Y are molar ratios of [TEG/TEOS] and $[TEOS/M^{3+}]$ salt, respectively.

FT-IR spectra were recorded using a Bruker Equinox-55 FT-IR spectrometer. The spectra were collected in the range 4000−400 cm^{-1} with a resolution of 2 cm^{-1}. Solid samples were finely ground and dispersed in spectroscopic grade potassium bromide. The disks were vacuum-dried at 70 °C for 7 days before the experiment.

The cells used in the present studies have the configuration SS/ormolyte/SS, where SS refers to stainless steel and ormolyte refers to the solid electrolyte. Impedance measurements were carried out using Autolab electrochemical system II PGSTAT30 (Ecochemie, The Netherlands). The impedance measurements were carried out in the frequency range of 10^6−1 Hz with an applied ac bias of 50 mV rms to determine the conductivity parameters. The temperature range used was from 25 to 80 °C. The electrode samples were monoliths of thickness ranging between 0.5 and 1 mm. The electrical contact between the sample and the symmetric stainless steel disk electrodes (area 0.502 cm^2) was achieved using conductive silver paste (Eltecks Corp., India). Before impedance measurements, all the samples were kept at 80 °C in a vacuum for 7 days to remove the residual solvent and water. Prior to initiating the measurements, the samples were heated in dynamic vacuum at 100 °C for 3 h.

III. Results and Discussion

The sol−gel derived PEG−silicate composites containing europium triflate salt are transparent, mechanically strong, free-standing monoliths with thickness ranging between 0.5 and 2 mm. The physicochemical characterization based on the thermal analysis, NMR, and XRD reveals that the matrix can be best described as diphasic with silicate as fillers in the organic phase that provides solubility of the ionic dispersants.[4] It is expected that the presence of organic−inorganic interface may assist in the solvation of ions and let them be present as "free ions". The free ion concentration in a solid electrolyte should be high in order to achieve good ionic conductivity. However, there is a tendency to form ion pairs and aggregates depending on the salt concentration in the matrix, whenever triflate salts are used.[24] Since the formation of ion pairs and aggregates play a decisive role in the ionic conductivity of solid electrolytes, it is very essential to understand the nature of species present and their relative contribution to the observed conductivity.

A. Vibrational Spectroscopy. In general, polymeric materials having low dielectric constants ($\epsilon < 20$) lead to extensive ion−ion interactions. Raman and IR spectroscopic studies have confirmed the presence of strong ion−ion interactions in polymer electrolytes.[1,24−26] Raman spectroscopic results obtained for solvated free ions have been used to interpret the conductivity data.[1,24,25]

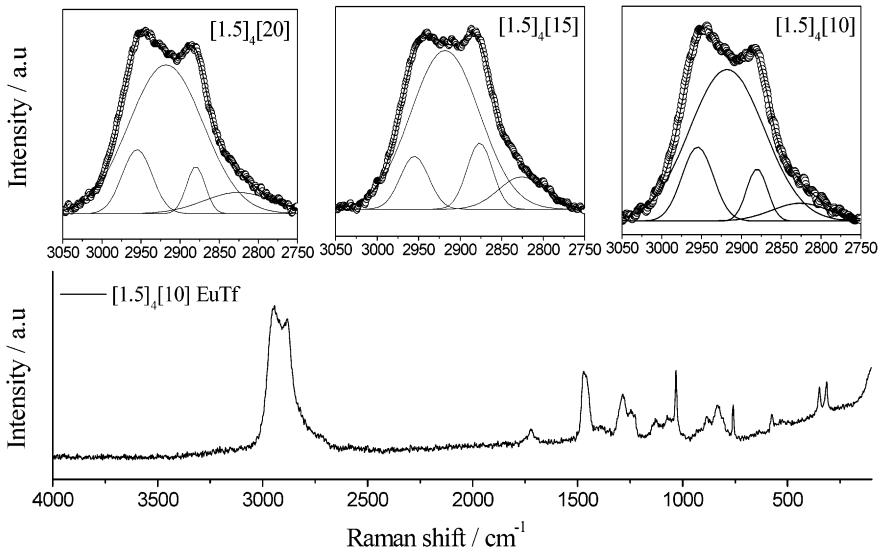

Figure 1. FT-Raman spectra of the ormolytes containing EuTf. The compositions are given in the figure. The deconvolution of the CH_2 symmetric stretching mode for different compositions of the ormolyte is shown at 25 °C.

The internal vibrations of anions such as perchlorate (ClO_4^-) and triflate ($CF_3SO_3^-$)[27,28] show a clear distinction between free ions and contact ion pairs or ion clusters. However, the free ions and solvent separated ion pair are difficult to distinguish from the spectroscopic data. Vibrational spectroscopy can detect short-lived ionic aggregates that are in dynamic equilibrium with free ionic species and the coordination sites of the polymer backbone or different ionic species. The time scale involved in vibrational spectroscopy is of the order of $10^{-12}-10^{-14}$ s and is several orders of magnitude faster than the typical conductivity and dielectric spectroscopy time scale. In the present study, we have used both vibrational and impedance spectroscopies to characterize the ormolytes.

The "short-range conformational disorder" is probed using the low-frequency region of the Raman spectra. The disordered longitudinal acoustic mode (D-LAM) occurs at frequencies below 300 cm^{-1} in the Raman spectrum.[29,30] This band reflects the measure of disorder in a polymer matrix. However, in the case of trivalent cation containing ormolytes, the intense bands of $\rho(SO_3)$ at 350 cm^{-1} and $\nu_s(C-S)$ at 315 cm^{-1} mask the D-LAM band.

High-Frequency Region (3050−2750 cm^{-1}). The Raman spectra of ormolytes containing triflate of Eu^{3+} cation with different salt concentrations in the region 3050−2750 cm^{-1} are presented in Figure 1. A representative spectrum in the whole range is also shown for one of the compositions. The deconvoluted spectra show the complex nature of interactions observed in the matrix. The bands at around 2950 and 2920 cm^{-1} correspond to the asymmetric CH_2 stretching vibration of the ordered chain conformation (- -O-trans-C-gauche-C-trans-O- -) and the disordered chain, respectively,[31] while the band at around 2880 cm^{-1} corresponds to the symmetric CH_2 stretching vibration. It is very clear that the intensity of the disordered band is higher than the intensity of the ordered band. The ratio of the area under the peak of the disordered band to the area under the peak of the ordered band is taken to be a measure of relative population of the disordered to the ordered conformers (Table 2). The disorder/order ratio decreases for both series of ormolytes, revealing that the system gets more ordered as a function of increasing salt concentration. It may be speculated that the cation coordination to the ether oxygen atoms in the ethylene glycol units may lead ordered structure. Further, the decreased conformational freedom due to the cation cross-linking between oxygens of neighboring chains may also be attributed to the observed decrease in the order.

Table 2. Ratio of 2918 cm^{-1} to 2955 cm^{-1} Band for Different Salt Concentrations[a]

composition	salt	disorder (2918)/order (2955)
$[1.5]_4[20]$		5.75
$[1.5]_4[15]$		7.26
$[1.5]_4[10]$		4.87
$[1.5]_4[8]$		3.98
	$Eu(CF_3SO_3)_3$	
$[1]_4[30]$		6.15
$[1]_4[20]$		1.94
$[1]_4[15]$		3.56
$[1]_4[8]$		0.88

[a] The area under each band is calculated from the deconvoluted $\nu_s(CH_2)$ stretching region.

Ion Association. Polymer electrolytes containing trivalent cations are little understood in terms of ion aggregation phenomena.[7,8] The earlier spectroscopic investigations on the trivalent ion containing solid electrolytes reveal that the free ion fraction is small at all concentrations of the salt, and consequently ion pair has been observed as a major component.[7,8] It is also speculated that the polymer is not able to solvate the trivalent cations, and as a result undissociated salt is present in the matrix. This observation would have a large effect on the ionic conductivity of the solid electrolytes. In the present study, a composite of silicate and poly(ethylene glycol) is used as the matrix, and it is believed that the glycol units in the presence of silicate domains may lead to a large fraction of free ions.

The use of band area analysis as a probe of the relative percentage of concentration of various ionic species is very common in the literature. However, it should be noted that Raman scattering cross sections might not be the same for the original band and the shoulders/satellites, etc., especially when the symmetry is lowered. The data that can be obtained without a correction for the sum of all the bands with the salt concentration is a relative decrease or increase in the

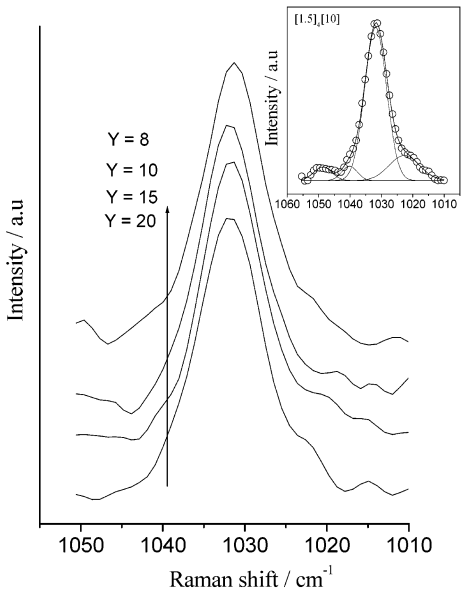

Figure 2. FT-Raman spectra for symmetric SO_3 stretching mode of EuTf-based ormolytes. Spectra are artificially stacked for clarity. The deconvoluted spectra of composition $[1.5]_4[10]$ is shown as inset. The arrow shows the position of 1039 cm^{-1} where the ion pair is expected.

Table 3. Band Assignments for Triflate Species[34]

band	wavenumber (cm^{-1})	assignment
$\nu_s(SO_3)$	1032	free ion/solvent-separated pairs
	1040	ion pairs
	1051	higher aggregates
$\nu_a(SO_3)$	1272	free ions
	1255, 1304	ion pairs
	1248	higher aggregates
	1290	higher aggregates

population of various ionic species. The symmetric (SO_3) stretch in triflate anion is nondegenerate, and hence its spectral shape is expected to be a simple Lorentzian[32−35] with a fwhm ∼ 5 cm^{-1}. Any broadening of this band leads to a conclusion that there are other possible electronic structures present. Figure 2 shows the Raman spectra of the ormolytes containing europium triflate salt in the symmetric (SO_3) stretching frequency range. The fwhm of the deconvoluted free triflate in the present studies is ∼8 cm^{-1} for all the compositions. The band positions are assigned (Table 3) according to the reported literature values.[34] The assignments are based on studies using the ab initio self-consistent Hartree−Fock method as well as the experimental observations.[34] The spectra show maximum intensity at 1032 cm^{-1} with a weak shoulder at 1039 cm^{-1} in all the compositions studied. The bands are assigned as 1032 cm^{-1} as free ion, ∼1039 cm^{-1} as ion pair, and ∼1051 cm^{-1} as higher aggregates. The presence of the 1032 cm^{-1} band as a major component in the present study is a distinguishable feature compared to the literature reports. Brodin and co-workers[8] have followed the ion association phenomena in the case of europium triflate in poly(propylene oxide) matrices. It is concluded that there are extensive cation−anion interactions that lead to ion pair formation at all concentrations. Extensive interactions between the Eu^{3+} and triflate have also been observed in the other organic matrix, poly(propylene glycol) (PPG), and reported based on luminescent and impedance measurements.[7,8] Two different environments for the solvated cation have been proposed. The

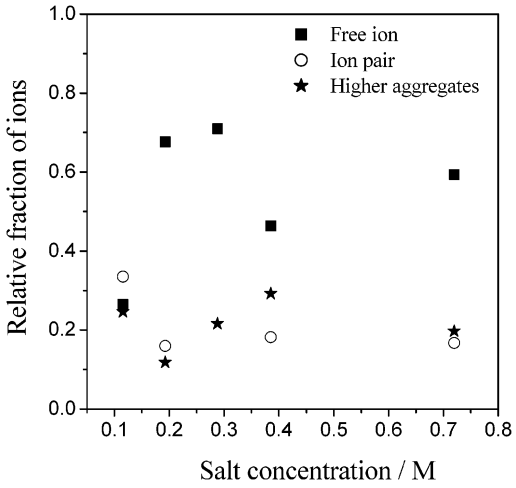

Figure 3. Fraction of different ionic species for ormolyte of EuTf. The composition used is $[1]_4[Y]$.

band observed at 1024 cm^{-1} may be attributed to the $\nu(CO)/\rho(CH_2)/\nu(C-C)$ mode.[36]

In the present study, the sol−gel based silicate−PEG matrix is able to minimize the cation−anion interactions and consequently show a large content of free ions in the matrix. It is speculated that the reason for this observation may be based on the "effective medium theory" proposed by Landauer.[37] According to this theory, fillers in organic matrices lead to a different surface charge at the organic−inorganic interface. The surface charge associated with this interface may result in a different ionic environment for the dissolved salt. In the present study, the interface between silicate and ethylene glycol units may result in the surface charge being conducive to the dissociation and stabilization of the free ions. This surface charge may facilitate the dissociation of high enthalpy trivalent triflate salt. The spectra are deconvoluted into three Gaussian functions (for free ion, ion pair, and higher aggregates) using a nonlinear least-squares fit method. The relative amounts of free ions/solvated ions (1032 cm^{-1}) and other higher aggregated species are given in Figure 3 for EuTf-based ormolytes as a function of the salt concentration. The free ion fraction increases with increasing salt concentration up to 0.3 M of the salt in the matrix. The concentration of the salt is given with respect to tetraethylene glycol unit. There is a decrease in the free ion fraction beyond this concentration. Simultaneously, the fraction of aggregates starts to increase, indicating that ion pairs or higher aggregates are formed at the expense of free ions. The relationship between the fraction of "free ions" and the ionic conductivity is discussed later.

The CF_3 symmetric deformation mode is one of the sensitive modes that gets affected by the cation−anion interactions in the case of triflate-based salts. However, it should be pointed out that the analysis of $\delta_s(CF_3)$ mode is difficult since it is observed with some contribution from the C−S stretching vibration as well.[38,39] Hence, it may not reflect the variations in the fraction of ionic species correctly. The spectrum corresponding to the europium-based ormolytes in the region of $\delta_s(CF_3)$ mode (not shown) reveals a single band due to the $\delta_s(CF_3)$ mode, probably coupled with the C−S stretch. The deconvoluted spectra show peaks at 752, 758, and 767 cm^{-1} that are assigned to free ions, ion pairs, and higher aggregates, respectively. The assignment is

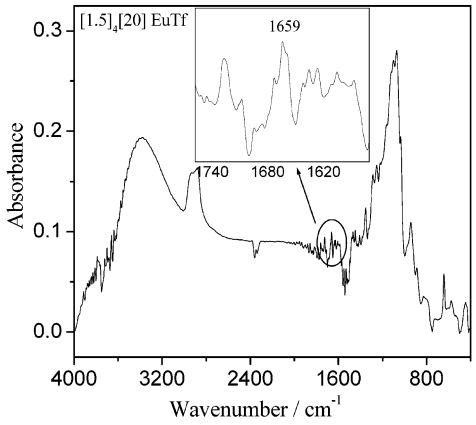

Figure 4. FT-IR spectra of ormolyte containing EuTf in the 4000−400 cm^{-1} frequency range. Inset shows the presence of the 1659 cm^{-1} band.

based on the observed spectral positions reported for lithium triflate based solid electrolytes.[32,34]

FT-IR Spectroscopy. The IR modes observed for the sol−gel derived silicates are broad and generally mask the bands due to other species. In the present studies, the FT-IR spectra of the as-prepared europium triflate containing ormolyte reveal the absence of bands that are characteristic of ethoxy groups (around 1190, 1056 cm^{-1}), indicating that the polymerization of the silane is complete (Figure 4). The presence of a dominant band around 1080 cm^{-1} is due to the formation of linear siloxane network (Si−O−Si).[40] A band observed at ~1659 cm^{-1} may be attributed to a combined effect of bonding of a water molecule with Eu^{3+} ion through the Eu^{3+}- -OH_x and also with an ethereal oxygen of PEG through H−O−H- - -O(PEG) bonding.[41] It is possible that the small dimension of europium ions (0.947 Å) may be unfavorable to directly bind with the ethylene oxide units that would not be sufficiently flexible to offer the ethereal oxygen atoms to the coordination sites of the metal ion. It is probably reasonable to assume that the interaction of tetraethylene glycol with the metal ion is through water molecules as given above.[41] The intensity of the O−H stretch occurring at the 3400 cm^{-1} band decreases as the sample is treated in a vacuum at an elevated temperature of 80 °C (not shown). However, a small peak is retained even after 7 days of vacuum treatment at 60 °C, and this is likely to be due to the uncondensed silanol O−H groups and the chemically bound water molecules as shown above.

The FT-IR studies are confined to the $[1.5]_4[Y]$ composition. The bands due to the polymerized silicate mask the other bands when the X value is below 1.5. At this composition, the bands due to other vibrations such as PEG−cation interactions are still observable. The spectra are corrected for the background and further deconvoluted assuming a Gaussian function, using the nonlinear least-squares fit method. In the case of ormolytes without salt, $[1.5]_4[0]$, the hydroxyl stretching mode, ν(OH), can be decomposed into three components as 3512, 3406, and 3256 cm^{-1}, corresponding to ν_a(OH), ν_s(OH), and ν_{hydro}(OH) stretching modes, respectively.[42] The hydroxyl groups involved in the analysis may be either due to the uncondensed silanols of the sol−gel derived silicate or due to the PEG phase. The ν_{hydro}(OH) band may be due to the OH stretching mode that is hydrogen bonded to another $(PEG)_4$ unit, and ν_a(OH), ν_s(OH) are the asymmetric and symmetric mode of terminal OH groups. Di Noto and co-workers[42] have

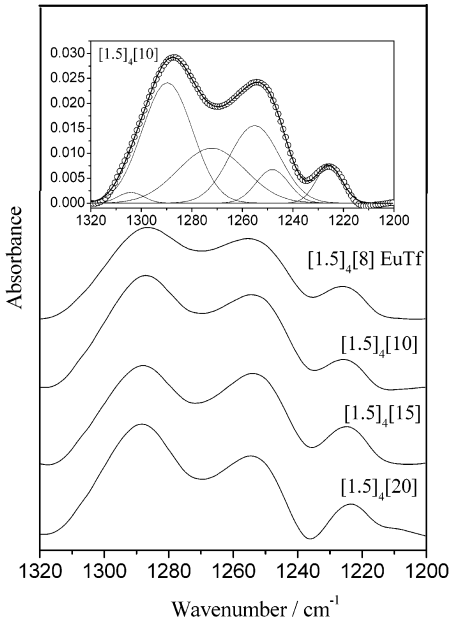

Figure 5. FT-IR spectra of ormolytes containing EuTf in the SO_3 antisymmetric and symmetric CF_3 stretching regions for different salt concentrations. The spectra are artificially stacked for clarity. The compositions are given in the figure. The deconvoluted spectrum is shown for one composition.

reported that the symmetric and asymmetric OH stretching modes are observed at 3605 and 3480 cm^{-1}, respectively, for "free" poly(ethylene glycol) (PEG-400). The "free" PEG spectrum is taken with low concentration of PEG dissolved in CCl_4 where the interactions between solute molecules are broken.[42] The "pure" PEG without a solvent has been reported to show bands at 3494 and 3335 cm^{-1} for the ν_a(OH) and ν_s(OH) modes, respectively. The shift in the positions of the two bands has been attributed to the effect of hydrogen bonding.[43−45] In a related study, it has been reported that a shift of 50 cm^{-1} in the OH stretching frequency in aqueous solutions corresponds to an increase in the hydrogen bond strength by roughly 1 kcal/mol.[43] Our spectral results indicate that there are shifts in the frequency of the OH stretch to the lower frequency region compared to the "free" PEG. This may be due to the presence of intramolecular hydrogen bonding as described earlier. If this empirical rule is applied in the present case, it would come to a hydrogen bond strength of 1.86 kcal/mol. It is of interest to note that the hydrogen bond strength is less the value of 2.55 kcal/mol reported for pure PEG.[42]

The IR spectra are analyzed in the spectral region where vibrational modes of the base matrix (SiO_2−PEG) are almost silent. The $\nu_a(SO_3)$ stretching region of the IR spectra of the europium triflate containing ormolytes is shown in Figure 5. Three main bands at 1290, 1255, and 1225 cm^{-1} are observed, and band intensities increase with increasing salt concentration. The deconvoluted spectra (shown in Figure 5) show bands at 1304, 1290, 1272, 1248, and 1225 cm^{-1}. The band analysis results are summarized in Table 3b. The band observed at 1225 cm^{-1} is recognized as the $\nu_s(CF_3)$ mode. The asymmetric SO_3 stretching mode of the isolated triflate ion is doubly degenerate. In the presence of sufficiently large cation−anion interactions, the axial symmetry of the anion is not preserved, and hence the SO_3 stretching mode will split into two components as the degeneracy is lifted. According to a previous study, the $\nu_a(SO_3)$ band

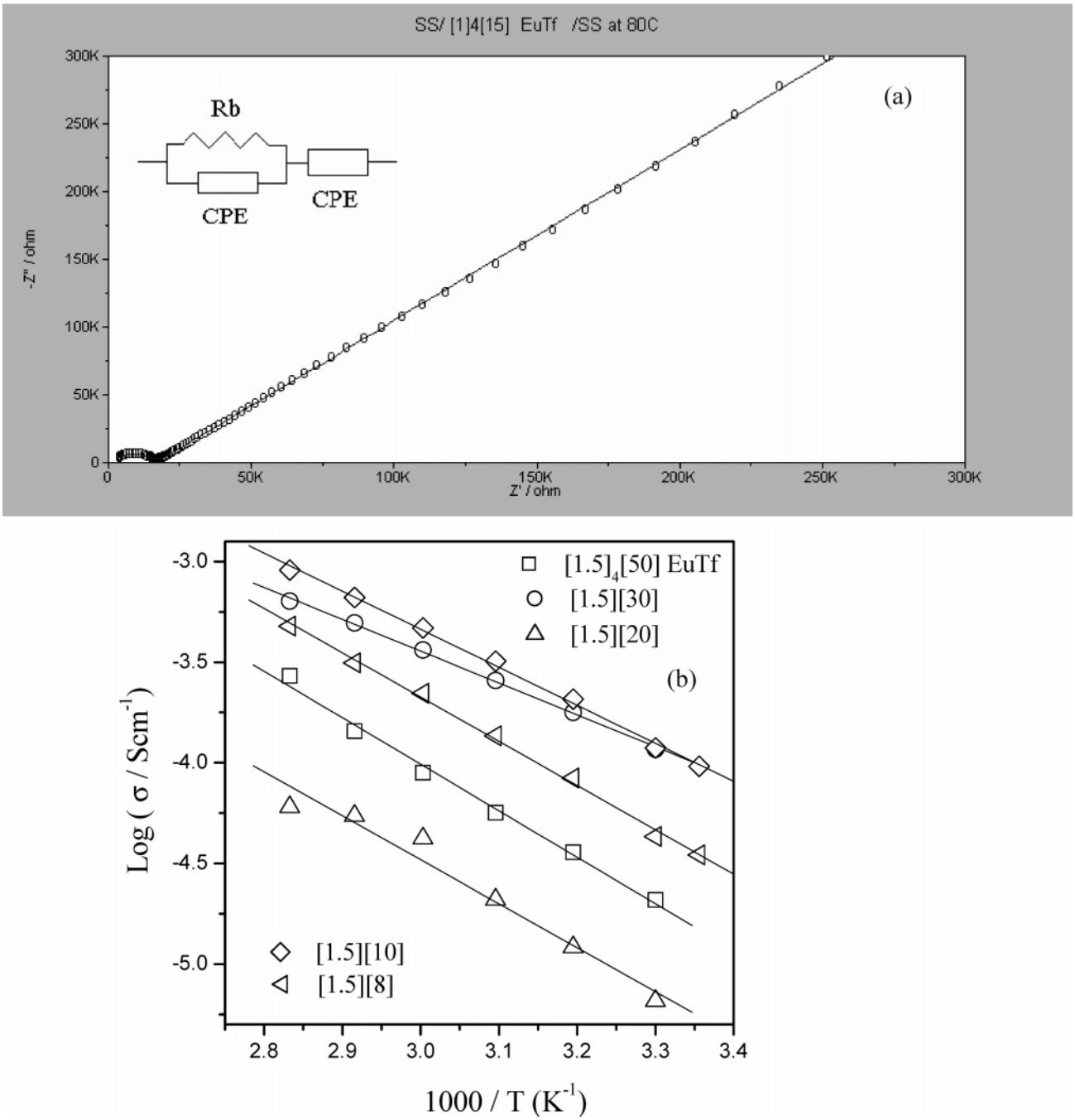

Figure 6. (a) Nyquist plot for ormolyte with EuTf at 80 °C. The composition is given in the figure. The SS electrodes used in the cell are of the area 0.502 cm^2. Open circles are experimental data, and the solid line through the open circles is fitted spectrum. (b) Temperature-dependent ionic conductivity plot for ormolytes containing EuTf. Open symbols are experimental data and solid lines through the open symbols are the fit to the Arrhenius equation. The compositions of the ormolytes are given in the figure.

for a noncoordinated (free ion) triflate ion is observed at 1274 cm^{-1} in acetonitrile solvent.[48b] The degenerate band is split into two bands upon interaction of the cation with the anion and is reported to occur at 1259 and 1301 cm^{-1}. These are reported to be due to ion pairs. The frequency difference between two components is reported to be the measure of the relative strength of cation−anion interaction.[48c] It is clear that there are two types of higher aggregates present in the case of ormolytes used in the present study. This is similar to the reported system based on LiTf in a copolymer of ethylene oxide and propylene oxide.[48b]

B. Ionic Conductivity. Impedance spectroscopy has been used to determine the ionic conductivity of the ormolytes containing europium triflate. The impedance studies are carried out using symmetric cells with stainless steel electrodes sandwiching the ormolyte. Typical Nyquist plots for selected composition of the ormolytes, in the frequency range 1 MHz−1 Hz, are shown in Figure 6a. A careful observation indicates the presence of semicircular arc at high frequencies that are attributed to the bulk properties of the ormolytes. The total impedance spectra can be fitted with bulk resistance and constant phase element (for bulk capacitance) in parallel with constant phase element (for interfacial capacitance) in series. Figure 6 shows the experimental impedance plot and the fit obtained from the equivalent circuit. The geometric capacitance values obtained from the high-frequency region, 10^6−10 Hz, are of the order of 10^{-12} F and are found to be independent of temper-

Table 4. Best Fit Parameters to Arrhenius Equation for dc Conductivity of the Ormolytes

compositions	$-\log(\sigma_0/\mathrm{S\ cm^{-1}})$	E_a (eV)
$[1]_4[100]$	3.15	0.19
$[1]_4[50]$	5.12	0.21
$[1]_4[30]$	7.31	0.26
$[1]_4[8]$	9.25	0.38
$[1.5]_4[50]$	2.92	0.20
$[1.5]_4[30]$	1.30	0.13
$[1.5]_4[20]$	2.06	0.18
$[1.5]_4[10]$	2.33	0.16
$[1.5]_4[8]$	2.93	0.19

ature and composition of the samples.[49] The low-frequency spike that is assigned to the effect of electrode−electrolyte interactions/electrode polarization[50] leads to capacitance values of 10^{-7} F. This value is found to be dependent on the temperature/composition and hence can be attributed to the interfacial phenomenon.

The semicircular arc shifts to lower impedance values with increasing temperature, indicating that the dc conductivity is a thermally activated process. The temperature-dependent dc conductivity values are calculated using the equation $\sigma = d/RA$, where the bulk resistance (R) is the diameter of the semicircular arc determined from the impedance spectra. Thickness of sample (d) is usually of the order of 0.2−0.5 mm, and the area (A) of the circular disk electrode is 0.502 cm^2 for all the experiments. The temperature dependence of dc conductivity for the ormolytes is shown in Figure 6b. The dependence follows an Arrhenius type of behavior. The Arrhenius-type dependence of ionic conductivity with temperature has been reported for trivalent cation-based solid polymer electrolytes[7,8,12,33] with other matrices. As will be shown later, the ac conductivity studies reveal that the ionic conduction is predominantly due to anion hopping. This may have its implications on the temperature dependence of ionic conductivity.

It is interesting to note that the observed ionic conductivity for PPG4000−EuTf solid electrolyte has been reported to be of the order of 3×10^{-8} S cm^{-1} at 30 °C.[7] The ormolyte exhibits a conductivity of $\sim 2 \times 10^{-5}$ S cm^{-1} for $[1.5]_4[50]$ composition at 30 °C. The activation energy (E_a) and the preexponential factor (σ_0) values, determined from the Arrhenius equation, as a function of salt composition are summarized in Table 4. The activation energies are found to be between 0.13 and 0.38 eV for $[1]_4[Y]$ and $[1.5]_4[Y]$ compositions of the ormolytes. This is lower than the reported value for PPG4000−EuTf composites (0.69 eV).[7] The ormolytes may contain larger fraction of amorphous domains than other electrolytes, resulting in low activation energies for ion transport.

The conductivity isotherm for europium triflate is given in Figure 7 as a function of salt concentration at 30 °C for $[1]_4[Y]$ composition. The ionic conductivity can be expressed in terms of cumulative contribution from various charge carriers, $\sigma = \sum n_m Z_m e \mu_m$, where n_m is the number of charge carriers of the type m, Z_m is the valence of the ionic species, e is the elementary electric charge, and μ_m is the ionic mobility. A strong dependence of ionic conductivity on the relative amounts of charge carriers and/or on the changes in the mobility of the various species with increasing salt concentration can be expected. It is evident from the figure that the conductivity reaches a maximum at concentrations of about 0.3 M (with respect to tetraethylene glycol), and

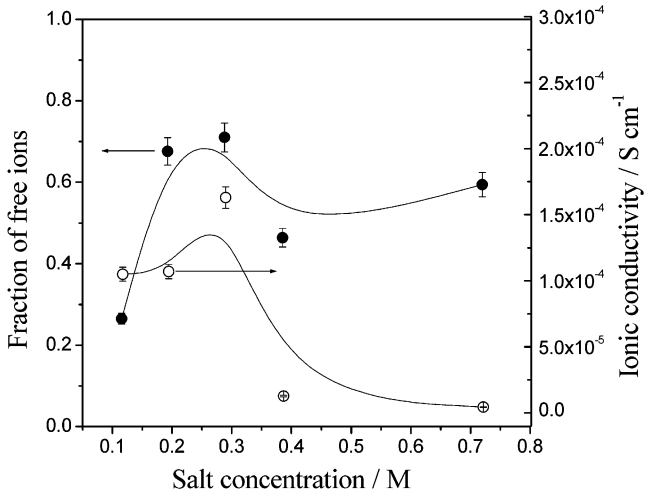

Figure 7. Fraction of the free ionic species calculated from $\nu_s(SO_3)$ stretching mode and ionic conductivity at 27 °C as a function of salt concentration for ormolytes containing EuTf. The solid lines are only guidelines to the eye.

then a decrease is observed. The formation of immobile aggregated species is responsible for this conductivity decrease at high salt concentrations.[51] In the case of trivalent cation containing systems, ion pairs and triplets will no longer be respectively neutral and charged as compared to the uni-univalent salt. Both species will carry a net residual charge, and the species can further coordinate to the PEG chains or to other free triflate anion by several ways. Therefore, the situation is more complicated than the mono- and divalent cation-based systems. It is of interest to note that the ionic conductivity variation is almost similar to the variation observed for the free triflate ion concentration as a function of salt concentration (Figure 7).

C. Frequency-Dependent Ionic Conductivity and Dielectric Behavior. In the present study, the ormolytes have been characterized over a wide range of frequencies, and the results are analyzed using on a combined approach based on a universal power law (UPL)[52] in the framework of jump relaxation model[53] and by an equivalent circuit analysis.

The ac conductivity is described using the power law proposed by Jonscher.[52a] Almond and West[54] have developed a formalism based on Jonscher's power law for the frequency dependence of conductivity of solid ionic conductors in the form $\sigma(\omega) = \sigma(0) + A\omega^n$, where "$A$" and "$n$" are temperature-dependent material parameters and $\sigma(\omega)$ is the ac conductivity at the frequency ω. The value of n is limited as $0 < n < 1$, and $\sigma(0)$ is the dc conductivity of the matrix. The use of UPL and equivalent circuit analysis has already been proposed for the analysis of ac impedance data in the case of systems containing lithium salts[55] and magnesium salts[2] in PEG matrices. The power-law equation, however, is not valid throughout the experimental frequency range since it does not include electrode polarization effects. The low-frequency region (generally below several tens of kilohertz) can be explained on the basis of the equivalent circuit as described earlier. The presence of electrode polarization at the low-frequency region in the case of ormolytes may be attributed to the high extent of dissociation of the salt and consequently the high conductivity. The low-frequency phenomenon develops with increasing temperature, and it implies that this may be coupled with the conductivity phenomenon.

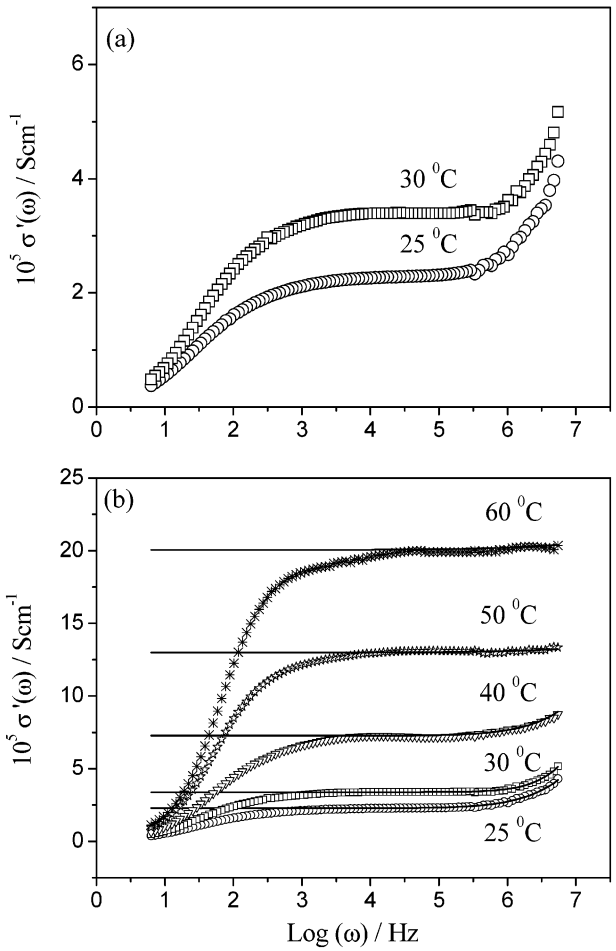

Figure 8. (a) Real part of conductivity $\sigma'(\omega)$ vs log(frequency) for ormolytes containing EuTf of composition $[1]_4[50]$ at 25 (○) and 30 °C (□). (b) Real part of conductivity $\sigma'(\omega)$ vs log(frequency) for ormolytes containing EuTf of composition $[1]_4[50]$ at different temperatures. Solid lines show the fitting of the UPL equation using the experimental data obtained at frequencies higher than 1 kHz.

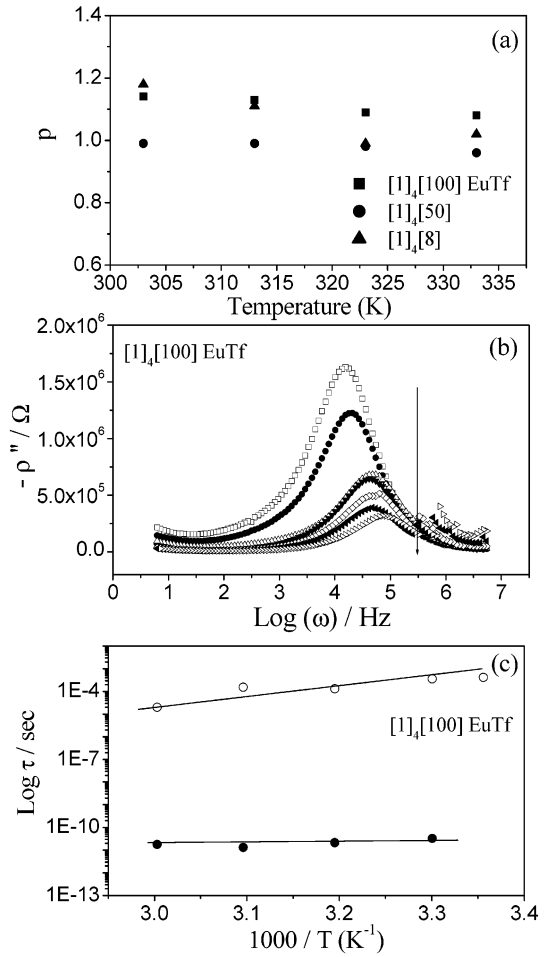

Figure 9. (a) Plot of $p(\tau_2/\tau^*)$ as a function of the temperature for ormolytes containing EuTf. The compositions of the ormolytes are given in the figure. (b) Imaginary component of the complex resistivity $-\rho''(\omega)$ vs log(frequency) for ormolytes containing EuTf at various temperatures. The arrow indicates the increasing temperature from 25, 30, 40, 50, 60, 70, and 80 °C. The composition is given in the figure. (c) Dependences of $\log(\tau_{peak})$ (○) and $\log(\tau_1)$ (●) on $1/T$ for ormolytes containing EuTf. Solid lines are the linear fit to the experimental data.

The analysis of the experimental data is carried out based on the jump relaxation framework model. This model states that the effective potential faced by a charged defect (in the present case, a migrating ion) is the summation of a periodic lattice potential and a "cage effect" potential caused by Coloumb interactions with other charge carriers. Accordingly, the events associated with ionic conduction will be (1) hopping of the charged species from one site to the another giving rise to ionic conductivity and (2) back-hopping to the initial site. This model allows us to probe the different time scales associated with ionic movement in the matrix. The experimental ac conductivity (real part) spectra are fitted using the following generalized UPL equation,[21,22,55] at frequencies higher than 1 kHz. The frequency-dependent conductivity is expressed as $\sigma'(\omega) = \sigma'(0)[1 + (\omega\tau_1)^p]$, where τ_1 is the time scale parameter which is related to initial site relaxation time for ion hopping τ_2 and the exponential parameter as $p = \tau_2/\tau^*$, and τ^* is the initial back-hop relaxation time. The fitting is carried out using the complex nonlinear least-squares method, and the solid lines in the figures are the fitted curves.

On the basis of spectroscopic results, it is believed that the salt is dissolved mostly in tetraethylene glycol units, and the organic phase is wrapped around the silicate network.[4,23] In general, for electrolytes with relatively high conductivity, the relaxation processes can be masked by the conductivity effect. The variation in the real component of ac conductivity, $\sigma'(\omega)$ as a function of frequency, for the europium triflate-based ormolytes is shown in Figure 8a. The real component of the conductivity is evaluated using the impedance data in the frequency range of 1 MHz−1 Hz as $\sigma'(\omega) = Z'(\omega)/k[(Z'(\omega))^2 + (Z''(\omega)^2)]$, where k is the cell constant and $Z'(\omega)$, $Z''(\omega)$ are the real and imaginary components of complex impedance. The real part of the ac conductivity shows dispersion behavior at all temperatures. The different regions observed are (a) the high-frequency spike at low temperatures that is attributed to the ionic motions in bulk electrolyte,[56−58] (b) the medium-frequency plateau due to the dc conductivity of the sample, and (c) the low-frequency dispersion due to the electrode−electrolyte interaction or space-charge polarization.[50] The presence of electrode polarization at low-frequency region is attributed to the high extent of dissociation and is in parallel with the large fraction of free ions and consequently the high conductivity of the ormolytes at high temperatures. The observation of high-frequency phenomenon is correlated to the long-

Table 5. Activation Energy and Preexponential Factor as a Function of Salt Concentration in the Ormolytes Containing EuTf[a]

concn ($C^{1/2}$, mol)	salt	$\tau_{0,1}$ log (s)	$E_{0,1}$ (eV)	$\tau_{0,p}$ log (s)	$E_{0,p}$ (eV)
0.24	EuTf	−16.8	0.08	−9.9	0.08
0.34	EuTf	−16.03	0.09	−7.37	0.05
0.85	EuTf	−12.26	0.04	−15.19	0.16

[a] The composition of the ormolyte is $[1]_4[Y]$.

range conductivity process or translational motion of the mobile ions. It is observed that the change in high-frequency dispersion with increasing temperature may be due to an increase in the ion migration rate.[51] The UPL equation was fitted to the experimental $\sigma'(\omega)$ spectra by varying the parameters $\sigma(0)$, τ_1, and p. The UPL equation fits are shown as the solid lines passing through the experimental points (open circles) represented in Figure 8b and reveal that the ac conductivity spectra satisfy the UPL above 1 kHz frequency. Below 1 kHz frequency, the electrode polarization phenomenon predominates, and hence the fit is not proper. The observed electrode polarization effect increases with increasing temperature (Figure 8a). The fraction of ions accumulating at the electrode−electrolyte surface increases with temperature, resulting in an increase in the interfacial capacitance. The best-fit parameters $\sigma(0)$, τ_1, and p are used for further analysis.

At this point, it is important to analyze the parameter "p" as a function of temperature. The parameter "p" is defined as the ratio of initial site relaxation time to the time for the back-hopping event. Therefore, the overall conductivity of the bulk material will increase only when the time for initial relaxation process is greater than the back-hopping event time.

Figure 9a shows the parameter "p" as a function of temperature. It is observed that "p" is greater than one at 30 °C and tends toward one at high temperatures. Therefore, at low temperatures, the overall conductivity may be due to anion hopping events or anion exchange between polymer bound cations and a higher aggregated cation−anion complex. At high temperatures, the aggregates may redissociate, giving rise to free cations, and this probably results in the "p" value being less than

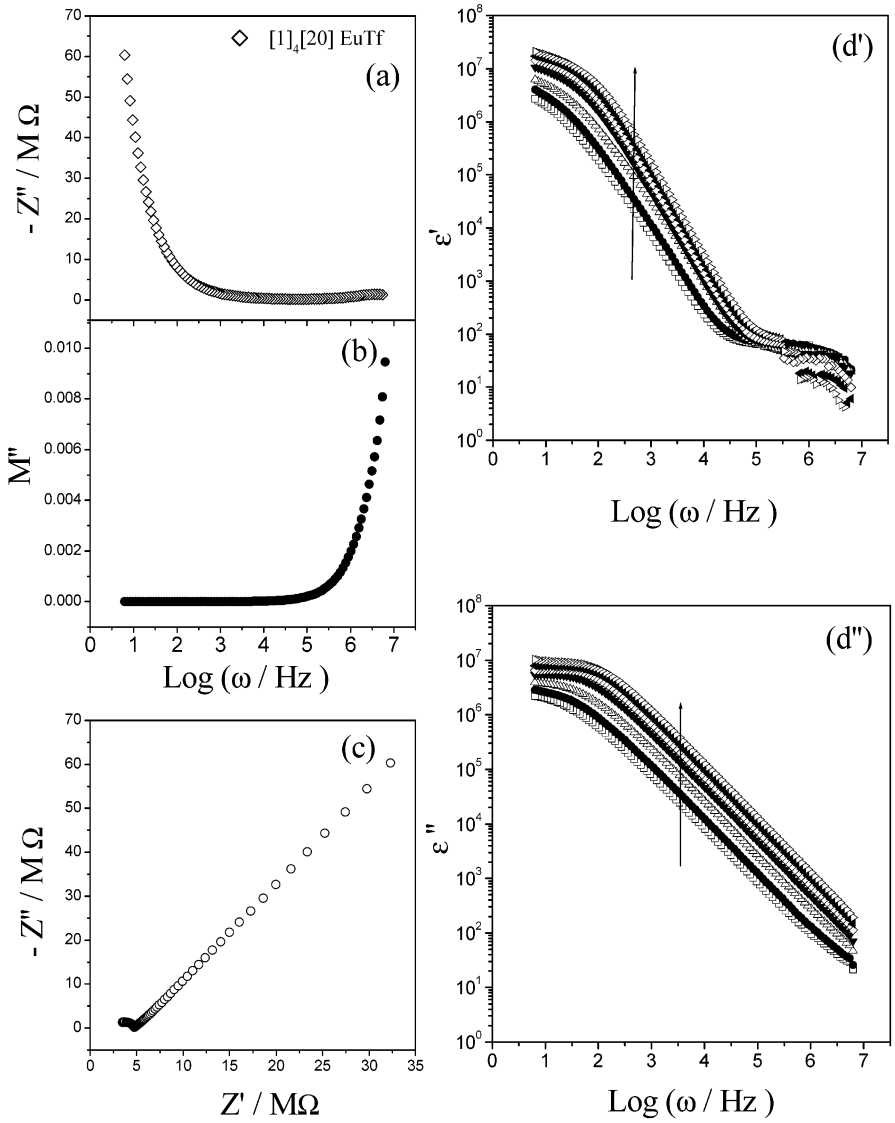

Figure 10. (a) Log(imaginary impedance) vs log(frequency), (b) electric modulus vs log(frequency), and (c) Nyquist plot for the ormolyte of composition $[1]_4[20]$ EuTf at 30 °C. (d′) Real component of complex dielectric permittivity as a function of log(frequency) for EuTf ormolyte of composition $[1]_4[100]$ at various temperatures. (d″) Imaginary component of complex dielectric permittivity as a function of log(frequency) for EuTf ormolyte of composition $[1]_4[100]$ at various temperatures. Arrow indicates increasing temperature from 25, 30, 40, 50, 60, 70, and 80 °C.

unity. Another parameter that can yield information on the conduction mechanism is based on the plot of $-\rho''(\omega)$ (imaginary part of resistivity) vs frequency. Figure 9b shows the plots of $-\rho''(\omega)$ vs frequency for the ormolytes. The typical Lorentzian-shaped Debye plots show the presence of peak maximum at all temperatures.[55] The maximum point is found to depend on the temperature, salt concentration, and the ormolyte composition. The profiles are fit using Lorentzian functions, and the fitting parameters give information on the conductivity relaxation time as $\tau_{peak} = 1/f_{peak}$.[55]

Additional information on the conductivity mechanism may be obtained by following the relaxation time, τ_{peak} and τ_1 (correlated with the initial site relaxation time τ_2), determined from the resistivity relaxation and UPL fitting to the ac conductivity, respectively. The two time scale parameters (τ_{peak} and τ_1) are plotted against temperature and are shown in Figure 9c. All the spectra show Arrhenius-type behavior according to the equations

$$\tau_{peak} = \tau_{0,peak} \exp[E_{a,peak}/RT]; \quad \tau_1 = \tau_{0,1} \exp[E_{a,1}/RT]$$

where $\tau_{0,peak}$ and $\tau_{0,1}$ are the preexponential constants and $E_{a,peak}$ is the activation energy related to the thermally activated ion motion and $E_{a,1}$ is the activation energy related to the barrier for the initial site relaxation process. The best-fit parameters are given in Table 5. The activation energies obtained from different plots show similar values for $E_{a,0}$ and $E_{a,peak}$ at the low-temperature range (25−60 °C) for all the cases. This indicates that the conductivity mechanism is likely to be based on ion hopping, and the processes are thermally activated.

The high-frequency dispersion behavior of real part conductivity has been often related to the universal dielectric response (UDR) for dielectric materials in the literature. [52a] This has been extended to conductive systems as the "universal dynamic response". The two coupled phenomena are difficult to separate since both give rise to the same geometric capacitance value. According to Gerhardt,[59] plots of impedance and electric modulus with frequency are extremely helpful in distinguishing between the localized and delocalized relaxation in the bulk. Figure 10a,b shows the $-Z''$ vs frequency and M'' vs frequency plots for the ormolytes at 30 °C. The temperature 30 °C is chosen where a complete detectable semicircle is obtained, and the dc conductivity contribution is very low, leading to undisturbed ac relaxation behavior. Both $-Z''$ vs frequency and M'' vs frequency representations show dispersion, and there is no relaxation peak observed in M'' (electric modulus) spectra. The absence of a peak in the imaginary part of the dielectric parameter suggests that long-range conductivity is predominant over dielectric functions. This is supported by the data of complex impedance shown in Figure 10c.

Dielectric behavior of ormolytes is examined in the same frequency range. The variations of dielectric constants and electrical modulus are also shown in Figure 10. The dispersion in the electrical modulus spectra is quite typical of dielectric loss. The high values of ϵ' observed for the trivalent cation-based ormolytes is due to the enhanced charge carrier density at the space charge accumulation region, resulting in an increase in the equivalent capacitance. The loss behavior is mainly due to the high ionic conductivity of the matrix that masks the relaxation behavior.

IV. Conclusions

The detailed characterization of ormolytes containing europium triflate have been carried out using FT-Raman, FT-IR spectroscopy, and ac conductivity measurements. FT-Raman of the ormolytes reveals the existence of large fraction of spectroscopically free triflate anion in addition to ion-pair and higher aggregates. The fractions of ion-pair and higher aggregates increase with increasing salt concentration. Temperature-dependent ionic conductivity reveals pure Arrhenius-type behavior, and the origin of this behavior has been investigated by analyzing the frequency-dependent conductivity and electric modulus representations. The ac conductivity response for these ormolytes is carried out using equivalent circuit and correlated ionic motion analysis based on the "universal power law" equation, related to the "jump relaxation model" framework. Analysis of $\sigma'(\omega)$ with angular frequency suggests that the "p" parameter is greater than unity in most of the cases. This observation leads to the fact that the back-hopping process occurs at a higher rate than initial site relaxation event. The ion migration may be due to hopping of anion among species like Eu^{3+}/$[EuTf]^{2+}$/$[EuTf_2]^+$ coordinated to the oxygen atoms of poly(ethylene glycol) units. Low activation energy observed for the ion migration process indirectly suggests anion hopping for the total charge migration under applied potential.

Acknowledgment. The authors thank the Ministry of Non-Conventional Energy Sources, New Delhi, for funding.

References and Notes

(1) Gray, F. M. In *Polymer Electrolytes*; RSC Materials Monographs; RSC; Cambridge, UK, 1997.
(2) Scrosati, B.; Neat, R. J. In *Applications of Electroactive Polymers*; Scrosati, B., Ed.; Chapman and Hall: London, 1993.
(3) Hug, R.; Chiodelli, G.; Ferloni, P.; Magistris, A.; Farrington, G. C. *J. Electrochem. Soc.* **1998**, *135*, 524.
(4) Mitra, S.; Sampath, S. *J. Mater. Chem.* **2002**, *12*, 2531.
(5) Girish Kumar, G.; Sampath, S. *J. Electrochem. Soc.* **2003**, *150*, A608.
(6) Girish Kumar, G.; Sampath, S. *Solid State Ionics* **2003**, *160*, 289.
(7) Ferry, A.; Furlani, M.; Franke, A.; Jacobsson, P.; Mellander, B.-E. *J. Chem. Phys.* **1998**, *109*, 2921.
(8) Brodin, A.; Mattsson, B.; Torell, L. M. *J. Chem. Phys.* **1994**, *101*, 4621.
(9) Di Noto, V.; Bettińelli, M.; Furlani, M.; Lavina, S.; Vidali, M. *Macromol. Chem. Phys.* **1996**, *197*, 375.
(10) Capobianco, J. A.; Proulx, P. P.; Raspa, N.; Simkin, D. J.; Krashkevich, D. *J. Chem. Phys.* **1989**, *90*, 2856.
(11) Carlos, L. D.; Videira, A. L. L. *Phys. Rev. B* **1994**, *49*, 11721.
(12) Silva, M. M.; De, V.; Bermudez, Z.; Carlos, L. D.; Almeida, A. P.; Smith, M. J. *J. Mater. Chem.* **1999**, *9*, 1735.
(13) Imanaka, N.; Kobayashi, Y.; Tamura, S.; Adachi, G. *Solid State Ionics* **2000**, *136−137*, 319.
(14) Croce, G. B.; Appetechi, L.; Perci, B.; Scrosati, B. *Nature (London)* **1998**, *394*, 456.
(15) Portier, J.; Choy, J. H.; Subramaniyan, M. A. *Int. J. Inorg. Mater.* **2001**, *3*, 581.
(16) Dias, F. B.; Plomp, L.; Veldhuis, B. J. *J. Power Sourses* **2000**, *88*, 169.
(17) Agrawal, R. C.; Gupta, R. K. *J. Mater. Sci.* **1999**, *34*, 1131.
(18) Ravaine, D.; Seminet, A.; Charbonillit, Y.; Vincens, M. *J. Non-Cryst. Solids* **1986**, *82*, 210.
(19) Furukawa, T.; Imura, M.; Yuruzume, H. *Jpn. J. Appl. Phys.* **1997**, *36*, 1119.
(20) Furukawa, T.; Yoneya, K.; Takahashi, Y.; Ito, K.; Ohno, H. *Electrochim. Acta* **2000**, *45*, 1443.
(21) Di Noto, V. *J. Phys. Chem. B* **2000**, *104*, 10116.
(22) Di Noto, V. *J. Phys. Chem. B* **2002**, *106*, 11139.

(23) Judeinstein, P.; Titman, J.; Stamm, M.; Schmidt, H. *Chem. Mater.* **1994**, *6*, 127.
(24) Hyun, J.-K.; Dong, H.; Rhodes, C. P.; Frech, R.; Wheeler, R. A. *J. Phys. Chem. B* **2001**, *105*, 3329.
(25) Manning, R.; Frech, R. *Polymer* **1992**, *33*, 3487.
(26) Bakker, A.; Gejji, S.; Lindgeren, J.; Hermansson, K.; Probst, M. M. *Polymer* **1995**, *36,* 4371.
(27) Schantz, S.; Torell, L. M.; Stevens, J. R. *J. Chem. Phys.* **1991**, *94*, 6862.
(28) Rhodes, C. P.; Frech, R. *Solid State Ionics* **1999**, *121*, 91.
(29) Snyder, R. G. *J. Chem. Phys.* **1982**, *76*, 3921.
(30) Snyder, R. G.; Wunder, S. L. *Macromolecules* **1986**, *19*, 496.
(31) Shashikov, S.; Wartewig, S.; Sandner, B.; Tubke, J. *Solid State Ionics* **1996**, *90*, 261.
(32) Ferry, A. *J. Phys. Chem. B* **1997**, *101*, 150.
(33) Bernson, A.; Lindgren, J.; Huang, W.; Frech, R. *Polymer* **1995**, *36*, 4471.
(34) Huang, W.; Frech, R.; Wheeler, R. A. *J. Phys. Chem.* **1994**, *98*, 100.
(35) Rhodes, C. P.; Kiassen, B.; Frech, R.; Dai, Y.; Greenbaum, S. G. *Solid State Ionics* **1999**, *126*, 251.
(36) Quartarone, E.; Tomasi, C.; Mustarelli, P.; Magistris, A. *Electrochim. Acta* **1998**, *43*, 1326.
(37) Landauer, R. *J. Appl. Phys.* **1952**, *23*, 779.
(38) Varetti, E. L.; Fernandez, E. L.; Ben Altabef, A. *Spectrochim. Acta* **1991**, *47A*, 1767.
(39) Miles, M. G.; Doyle, G.; Cooney, R. P.; Tobias, R. S. *Spectrochim. Acta* **1969**, *25A*, 1515.
(40) Buining, P. A.; Humbel, B. M.; Phillose, A. P.; Verkleji, A. J. *Langmuir* **1997**, *13*, 3921.
(41) Horikoshi, K.; Hata, K.; Kawabata, N.; Ikawa, S. *J. Mol. Struct.* **1990**, *239*, 33.
(42) Di Noto, V.; Longo, D.; Muenchow, V. *J. Phys. Chem. B* **1999**, *103*, 2636.
(43) Joesten, M. D.; Drago, R. S. *J. Am. Chem. Soc.* **1962**, *84*, 3817.
(44) Drago, R. S.; O'Bryan, N.; Vogel, G. C. *J. Am. Chem. Soc.* **1970**, *92*, 3924.
(45) Kanno, H.; Hiraishi, J. *J. Raman Spectrosc.* **1987**, *18*, 157.
(46) Bernson, A.; Lindgren, J. *Polymer* **1994**, *35*, 4842.
(47) Frech, R.; Huang, W. *J. Solution Chem.* **1994**, *231*, 469.
(48) (a) MacFarlane, D. R.; Meakin, P.; Bishop, A.; MacNanghton, D.; Rosalie, J. M.; Forsyth, M. *Electrochim. Acta* **1995**, *40*, 2333. (b) Bishop, A. G.; MacFarlane, D. R.; McNanghton, D.; Forsyth, M. *J. Phys. Chem.* **1996**, *100*, 2237. (c) Frech, R.; Chintapalli, S.; Bruce, P. G.; Vincent, C. A. *Macromolecules* **1999**, *32*, 808.
(49) Bruce, P. G. In *Polymer Electrolyte Reviews 1*; MacCallum, J. R., Vincent, C. A., Eds.; Elsevier Applied Science: New York, 1987.
(50) Heumen, J. V.; Wieczoreck, W.; Siekierski, M.; Stevens, J. R. *J. Phys. Chem.* **1995**, *99*, 15142.
(51) Hall, P. G.; Davies, G. R.; McIntyre, J. E.; Ward, I. M.; Bannister, D. J.; LeBroeq, K. M. F. *Polym. Commun.* **1986**, *27*, 98.
(52) (a) Jonscher, A. K. *Dielectric Relaxation in Solids*; Chelsea Dielectrics: London, 1983. (b) Di Noto, V.; Barreca, D.; Furlan, C.; Armelao, L. *Polym. Adv. Technol.* **2000**, *11*, 1.
(53) Funke, K. *Z. Phys. Chem. (Munich)* **1995**, *188*, 243.
(54) Almond, D. P.; West, A. R. *Solid State Ionics* **1986**, *18/19,* 1105.
(55) Di Noto, V.; Vittadello, M.; Lavina, S.; Fauri, M.; Biscazzo, S. *J. Phys. Chem. B* **2001**, *105*, 4584.
(56) Lonergan, M. C.; Perran, J. W.; Ratner, M.; Shriver, D. F. *J. Chem. Phys.* **1993**, *98*, 4937.
(57) Lonergan, M. C.; Nitzan, A.; Ratner, M.; Shriver, D. F. *J. Chem. Phys.* **1995**, *103*, 3253.
(58) Roling, B. *J. Non-Cryst. Solids* **1999**, *244*, 34.
(59) Gerhardt, R. *J. Phys. Chem. Solids* **1994**, *55*, 1491.

MA0484328